Chemistry and Physics of Lipids 221 (2019) 198–206

Contents lists available at ScienceDirect

Chemistry and Physics of Lipids

journal homepage: www.elsevier.com/locate/chemphyslip

Reaction of ionised steryl esters with ozone in the gas phase

Sarah E. Hancock[a,b,1], Alan T. Maccarone[c,d], Berwyck L.J. Poad[e], Adam J. Trevitt[c], Todd W. Mitchell[a,b,*], Stephen J. Blanksby[e,**]

[a] School of Medicine, University of Wollongong, Wollongong, NSW, Australia
[b] Illawarra Health and Medical Research Institute, Wollongong, NSW, Australia
[c] School of Chemistry, University of Wollongong, Wollongong, NSW, Australia
[d] Mass Spectrometry User Resource and Research Facility, University of Wollongong, Wollongong, NSW, Australia
[e] Central Analytical Research Facility, Institute for Future Environments, Queensland University of Technology, Brisbane, QLD, Australia

ARTICLE INFO

Keyword:
Mass spectrometry
Lipid
Cholesterol
Oxidation
Ozone

ABSTRACT

Cholesterol is an ubiquitous membrane lipid, that also serves as a precursor to many steroid hormones. The 5,6 carbon-carbon double bond on the tetracyclic carbon backbone of cholesterol is an attractive target for ozone with the reaction giving rise to a wide range of possibly bioactive molecules. Despite this, little is known about the ozonolysis of cholesterol esters, which often possess an additional double bond(s) on the fatty acyl chain. Understanding the intrinsic gas phase reaction of ozone with the two disparate double bond positions on cholesteryl esters can inform our understanding of these processes *in vivo*, particularly reactions occurring at the air-water interface (*e.g.*, tear film lipid layer) and on the surfaces of the body where these cholesterol and cholesteryl esters may be present (*e.g.*, sebum). In the present work we describe the gas phase ozonolysis of lithium and sodium cations formed from three steryl esters: two isomeric for double bond position (cholestanyl oleate and cholesteryl stearate), and a third with carbon-carbon double bonds present in both the sterol ring system and fatty acyl chain (cholesteryl oleate). We confirm the enhanced reactivity of the endocyclic carbon-carbon double bond with ozone over double bonds present in the acyl chain, and elucidate competitive interactions between the two double bond positions during ozonolysis. Elucidation of the mechanisms underlying this interaction is important for both understanding these processes *in vivo* and for deploying ozonolysis chemistry in analytical strategies for lipidomics.

1. Introduction

Ozone is a chemically reactive oxidant present in the atmosphere that is hazardous to animal and plant tissues. It is most concentrated in the ozone layer of the stratosphere, where it has an important role in shielding the Earth's surface from harmful ultraviolet radiation. In the troposphere, ozone is a secondary pollutant formed from the action of sunlight on by-products of industry such as NO, CO, and volatile organic compounds (Finlayson-Pitts and Pitts, 2000). While typically present at levels in urban environments that are not harmful to humans and other animals (˜20-30 ppb), high levels of pollution and periods of hot weather can increase ground ozone concentrations to hazardous levels above 100 ppb. Sensitive external surfaces of the body, including the eyes, mucous membranes, and respiratory system are particularly vulnerable to the deleterious effects of ozone (Monks et al., 2015).

One of the ways ozone exerts its hazardous effects on human health is through reactions with biomolecules containing carbon-carbon double bonds, particularly unsaturated lipids (Pryor et al., 2006). The ozonolysis of cholesterol, an ubiquitous lipid with wide-ranging functions, has drawn much interest from both a biological and mechanistic perspective. Cholesterol belongs to the steroid class of lipids, which have tetracyclic saturated carbon rings as their core structural component. Sterols have a 3β-hydroxy group and an aliphatic side chain of 8 or more carbons attached at carbon 17, and cholesterol is unsaturated between carbons 5 and 6 on the B-ring of its steroid scaffold. Cholesterol is an essential component of animal cell membranes where it modulates membrane fluidity, and it serves as a precursor to various steroid hormones and bile acids (Nelson and Cox, 2008). The 3β-hydroxy present on cholesterol can be esterified with a fatty acid to form a cholesteryl ester, which are found either stored in intracellular lipid

* Corresponding author at: School of Medicine, University of Wollongong, Wollongong, NSW, Australia.
** Corresponding author at: Central Analytical Facility, Institute for Future Environments, Queensland University of Technology, Brisbane, QLD, Australia.
E-mail addresses: toddm@uow.edu.au (T.W. Mitchell), stephen.blanksby@qut.edu.au (S.J. Blanksby).
[1] Present address: School of Medical Sciences, University of New South Wales, Sydney Australia.

https://doi.org/10.1016/j.chemphyslip.2018.12.013
Received 26 September 2018; Received in revised form 20 December 2018; Accepted 27 December 2018
Available online 28 December 2018

droplets or packaged into lipoproteins for transport in plasma (Nelson and Cox, 2008). Cholesterol and/or cholesteryl esters also coat the surfaces of the body, being present in pulmonary surfactant (Pulfer and Murphy, 2004), skin (Hirabayashi et al., 2017), sebum (Camera et al., 2010), and the tear film lipid layer (Butovich, 2013). From a biological perspective, there is much interest in the range of bioactive oxysterols formed from cholesterol ozonolysis and their potential effects on human health (Hutchins et al., 2011; Pulfer et al., 2004, 2005; Pulfer and Murphy, 2004; Wentworth et al., 2003; Zhou et al., 2016). Cholesterol ozonolysis has also received much attention in mechanistic studies as its endocyclic double bond offers unique insight into ozonolysis reactions in both the gas (Dreyfus et al., 2005) and liquid phase (Gumulka et al., 1982; Gumulka and Smith, 1983; Jaworski and Smith, 1988; Paryzek et al., 1990; Ronsein et al., 2010). In comparison, little is known about the mechanism of ozonolysis of cholesteryl esters, which can contain two or more carbon-carbon double bonds: one between carbons 5 and 6 on cholesterol, and one (or more) in the acyl chain.

Despite being studied for close to 80 years, the mechanism underlying the ozonolysis of carbon-carbon double bonds is still not fully understood. It is commonly accepted that the dominant mechanism of alkene ozonolysis follows that described by Criegee (Criegee, 1975; Criegee and Wenner, 1949), where ozone adds across the carbon-carbon double bond in a concerted 1,3-cycloaddition forming a 1,2,3-trioxolane (or primary ozonide). The primary ozonide is short-lived and can degrade and undergo subsequent side reactions to yield a number of products, some of which are biologically active. Recent computational studies, however, point to two mechanisms for ozonolysis proceeding through (1) a transition state representing a concerted 1,3-cycloaddition, and (2) nucleophilic attack of ozone at one end of the alkene consistent with a step-wise addition across the double bond as previously proposed by DeMore (1969). Calculation of thermodynamic and kinetic barriers suggests that both mechanisms can compete effectively during ozonolysis depending on the physicochemical properties of the alkene, with factors such as steric hindrance, bond strain and bond length all contributing the dominant mechanism and corresponding ozonolysis products (Bailey and Lane, 1967; Chan and Hamilton, 2003; Krisyuk et al., 2016, 2013; Lee and Coote, 2013; Maiorov et al., 2008).

In the present study, we examined the reaction products and kinetics of gas phase ozonolysis of three ionised steryl esters: two are regioisomers that differ only by the site of unsaturation being located in either the sterol ring system (cholesteryl stearate) or acyl chain (cholestanyl oleate), and a third variant with a double bond present in both portions of the molecule (cholesteryl oleate). Our analysis demonstrates the enhanced reactivity of the endocyclic double bond in the cholesterol moiety compared with acyclic alkenes present in the acyl chain and provides evidence for a significant role of the charge-carrier in modulating the rate and product distribution in these ion-molecule reactions. Understanding the fundamental mechanism(s) of cholesteryl ester ozonolysis can inform our understanding of these processes *in vivo*, particularly with respect to ozonolysis reactions occurring at the air-water interface (*e.g.*, the tear film lipid layer).

2. Experimental

2.1. Materials

All solvents were of HPLC grade or higher, and were obtained from VWR International (Brisbane, QLD, Australia). Both lithium acetate and sodium acetate were of UHPLC grade, and were purchased from Sigma Aldrich (Sydney, NSW, Australia). Steryl esters were acquired from Nu-Chek Prep, Inc (Elysian, MN, USA), and included: cholesteryl stearate, cholestanyl oleate and cholesteryl oleate (Fig. 1). All three steryl esters were prepared as ~10 mM stock solutions in methanol, and were stored at −20 °C until use.

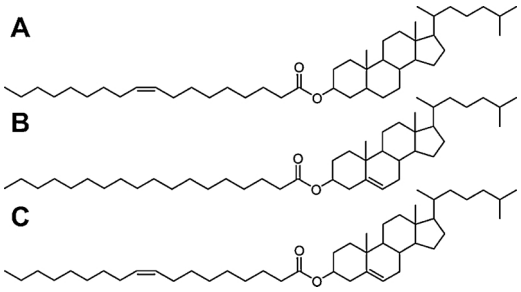

Fig. 1. Steryl esters used in the present study: cholestanyl oleate (A), cholesteryl stearate (B), and cholesteryl oleate (C).

2.2. Mass spectrometry

Ozone-induced dissociation (OzID) experiments were performed on a linear ion trap mass spectrometer (LTQ, Thermo Scientific, San Jose, CA, USA) equipped with an electrospray ion (ESI) source. The mass spectrometer was modified to allow the inline introduction of ozone into the helium bath gas in a similar manner to that previously described (Marshall et al., 2016; Thomas et al., 2008). Briefly, the helium collision gas supply to the ion trap was modified to allow external metering and blending-in of reagent gases (in this case ozone). An ozone generator (Titan 30, Absolute Ozone, Alberta, Canada) was used to produce ozone at either high or low concentrations in a stream of oxygen. Under high output (~225 g Nm^{-3}, 15% w/w O_2), ozone was produced from oxygen delivered at a flow rate of ~0.2 L min^{-1} with the potentiometer set at ~40%. For low ozone output (~40 g Nm^{-3}, 3% w/w O_2), oxygen was delivered at ~0.7 L min^{-1} with the potentiometer set at ~5%. Under both conditions, oxygen was delivered to the generator at a constant pressure of 20 psi. Delivery of ozone to the ion trap was controlled by a shut-off ball valve located upstream from a PEEKsil restriction line (10 cm × 25 µm) connected directly into the helium delivery line *via* a T-junction. Residual ozone was passed through a catalytic destruct prior to exhaust.

Steryl esters were prepared at 10 µM in methanol spiked with either lithium acetate or sodium acetate (to achieve concentrations of 1 mM and 50 µM, respectively) and directly infused into the mass spectrometer at a flow rate of 10 µL min^{-1}. Electrospray voltage was set at 4.5 kV and capillary temperature at 25 °C. Nitrogen was used as the sheath (7 arb units), auxiliary (0 arb units) and sweep (0 arb units) gases. Precursor ions were mass-selected at 2 Th, with a *q*-parameter of 0.25. For OzID experiments, the activation time parameter within the instrument control software was used to control the reaction time of the precursor ion with ozone; with activation (*i.e.* trapping) times varied systematically between 0.03–5000 ms. For collision-induced dissociation (CID) experiments, activation energy was typically set at 40–45 (arb units), with a default activation time of 30 ms. The MS^n capability of the ion trap was used to perform sequential CID/OzID or OzID/CID experiments. A minimum of 25 individual scans were acquired and averaged for all mass spectral data points. Analysis of meta-chloroperoxybenzoic acid (mCBPA)-treated cholesteryl stearate was conducted on an Orbitrap Elite mass spectrometer (Thermo Fisher Scientific, San Jose, CA) equipped with an automated chip-based nanoelectrospray source (TriVersa Nanomate™, Advion, NY, USA), which was modified to perform OzID experiments as described above. Ion-mobility measurements for the lithiated adducts were carried out using a traveling wave ion mobility mass spectrometer fitted with an electrospray ionisation source (SYNAPT G2-*Si*, Waters, Wilmslow, UK). All mass spectra were acquired between *m/z* 50 – 1200. Typical conditions for the experiment were: ESI caplillary voltage + 2 kV, desolvation temperature 400 °C and source temperature 120 °C. The samples were directly infused at a rate of 5 µL min^{-1}. Gas flow rates for the cone and desolvation gasses were set at 100 and 1000 L hr^{-1}, respectively. Collision energy (35 eV) was applied in the transfer region (*i.e.* after

TWIMS separation). A wave velocity ramp (1000 ms^{-1} to 300 ms^{-1}) was employed in the TWIMS cell to optimise separation. All other parameters relating to the travelling wave ion optics were set at their default values, with precursor ions being mass-selected with a window of 1 Da. The arrival time distributions of the lithiated acyl fragment (*m/z* 289 and *m/z* 291 for oleic and stearic acid, respectively) and steryl fragment (*m/z* 369 for cholesteryl, *m/z* 371 for cholestanyl) were used to infer the arrival time distribution of the respective steryl esters. To compensate for any mass-dependent mobility effects, the heavy isotope of cholesteryl oleate at *m/z* 659 (*i.e.*, isobaric with the $[M + Li]^+$ ions of the other two steryl esters) was used and the isotopic pattern of the respective fragments were extracted for comparison. All ion mobility spectra were acquired in successive runs on the same day within a 30 min interval to minimise any effects of changes in temperature and humidity on arrival time distribution.

2.3. Kinetics

Kinetic curves for the reaction of ozone with a given steryl ester ion were established in a similar fashion to that previously described (Prendergast et al., 2016). For each steryl ester as either $[M + Li]^+$ or $[M + Na]^+$, the *m/z* range of interest was integrated and normalised to the intensity of the total ion count, which was then plotted as a function of reaction time. Pseudo-first order rate constants (k_{1st}) were determined from fitting a least-squares estimate model using the Levenberg-Marquardt least-squares algorithm (Elzhov et al., 2016). Statistical uncertainty from fitting this model was calculated by first order Taylor expansion (Spiess, 2016). Second order rate constants (k_{2nd}) were determined from measured k_{1st} using the approximate ozone number density present within the ion trap at a given output from the external ozone generator. The reported theoretical second order rate constant for iodide ozonolysis (8.7×10^{-13} cm^3 molecules^{-1} s^{-1}) (Teiwes et al., 2018) was used to estimate the amount ozone present within the ion trap. Under high ozone output conditions, ozone concentration within the ion trap was estimated at 2.8×10^{11} molecules cm^{-3}, while low output resulted in 4.6×10^{10} molecules cm^{-3} of ozone. Reaction efficiencies were calculated from the measured k_{2nd} of given steryl ester ion as a percentage of the estimated collision rate calculated from a parameterized trajectory model (Su, 1994), using the dipole moment for ozone of 0.53 Debye and a polarizability of 3.21 Å (Khairallah et al., 2015; Lide, 2005; Miller, 2005). At least three kinetic curves were acquired for each steryl ester ion over successive runs.

3. Results and discussion

3.1. Gas phase ozonolysis of ionised cholestanyl oleate and cholesteryl stearate

Positive ion ESI mass spectrometry of cholestanyl oleate (Fig. 1A) within a methanolic solution spiked with either lithium or sodium acetate resulted in the production of abundant lithiated $[M + Li]^+$ or sodiated $[M + Na]^+$ precursor ions present at *m/z* 659 or *m/z* 675, respectively. Mass selection and trapping of these precursor ions in the presence of low concentration ozone (~4×10^9 molecules cm^{-3}) resulted the production of two main product ions in each case (Fig. 2A & B). The main product ion observed following this ozone-induced dissociation (OzID) reaction was detected 110 Da lower in mass than the precursor ion, with a second, less abundant ion also seen 94 Da below than the precursor ion. For cholestanyl oleate as $[M + Li]^+$, ozonolysis product ions were detected at *m/z* 549 and *m/z* 565, with each ion present at a relative abundance of 54.4% and 13.0%, respectively (normalised to a precursor ion abundance of 100%, Fig. 2A). Ozonolysis product ions from cholestanyl oleate as $[M + Na]^+$ were present at *m/z* 565 (3.3%) and *m/z* 581 (0.5%, Fig. 2B) but at a much lower abundance than in the $[M + Li]^+$ system. The *m/z* of these product ions is consistent with ozone-induced cleavage of the double bond between carbon-9 and carbon-10 of the oleic acid moiety (*i.e.*, the *n*-9 position, 9 bonds from the methyl end of the acyl chain) with either one or two oxygens remaining bound to carbon-9 as illustrated in Scheme 1. The presence of the additional oxygen on the truncated acyl chain was confirmed by re-isolation of the product ions and subsequent activation by both collision-induced and ozone-induced dissociation (Supplemental Material Figure S1 & S2). This pair of ozonolysis product ions is consistent with ozone-induced dissociation performed previously across a wide range of ionized lipids incorporating mono-unsaturated fatty acid substituents and indeed, the consistency of the neutral losses observed has been used extensively for the structural characterisation of lipids in complex extracts (Batarseh et al., 2018; Brown et al., 2011; Ellis et al., 2018; Hancock et al., 2018; Poad et al., 2018a, 2018b; Vu et al., 2017).

Similar gas phase ozonolysis experiments were performed for ionised cholesteryl stearate, which has a saturated acyl chain and a single carbon-carbon double bond located within the B ring of the sterol (Fig. 1B). Mass spectra arising from monitoring this reaction are shown in Fig. 2C & 2D for cholesteryl stearate ionised as $[M + Li]^+$ or $[M + Na]^+$, respectively. Isolation of these ions in the presence of ozone and allowing them to react for trapping times of up to 5000 ms led to the production of two main product ions. Irrespective of the adduct type, product ions were found to form 16 Da and 48 Da above the precursor ion while no significant product ions were identified at lower *m/z*. Regardless of the cation type, both the + 16 Da and + 48 Da cholesteryl stearate ozonolysis products appear to be end products, as they do not generate any further ions when sequentially reisolated and reacted with ozone (see Supplementary Material Figure S3). The structure of the +16 and +48 product ions from both lithiated and sodiated cholesteryl stearate were probed by CID. The resulting mass spectra are shown in Fig. 3 and all display abundant product ions representing a neutral loss of 284 Da (*e.g.*, *m/z* 391, Fig. 3C) that is consistent with expulsion of stearic acid and confirmatory evidence that the additional mass of oxygen is associated with the B ring and not the saturated fatty acyl motif. Interestingly, the results presented in Fig. 2C and D show that while the product ions are consistent between the two cations, the relative abundance distribution differs markedly. That is, for $[M + Li]^+$, the $[M + Li + 16]^+$ ion at *m/z* 675 is consistently more abundant than the $[M + Li + 48]^+$ ion at *m/z* 707 (Fig. 2C) while, in contrast, the main product ion observed from the ozonolysis of sodiated cholesteryl stearate was the $[M + Na + 48]^+$ ion at *m/z* 723.5 with the $[M + Na + 16]^+$ ion at *m/z* 691.5 present only in relatively low abundance; even after a 5000 ms reaction time. The reaction of ozone with lithiated cholesteryl stearate also appears to proceed much faster than that of sodiated cholesteryl stearate, with the precursor ion of the former being exhausted after only 500 ms of reaction time (Fig. 2C).

Prior studies of cholesterol ozonolysis in solution provide a number of possible proposals to account for the products observed from the gas phase reactions of ionised cholesteryl stearate with ozone. Possible reaction outcomes are outlined in Scheme 2 where addition of the ozone across the endocyclic double bond (either directly or stepwise) would give rise to a reactive primary ozonide (**2**) that can facilitate opening of the steryl B-ring to form either intermediates (**3a**) and (**3b**) that both incorporate the short-lived carbonyloxide moiety (the so-called Criegee intermediate). Literature precedent would indicate that the intermediates (**3**) could undergo rearrangement to yield, carboxylic acid (**4**), vinyl hydroperoxide (**5**), secondary ozonide (**6**) or lactone structures (**7**) (Dreyfus et al., 2005; Gumulka et al., 1982; Gumulka and Smith, 1983; Jaworski and Smith, 1988; Paryzek et al., 1990; Ronsein et al., 2010). All these possible product structures are isomeric and could account for the +48 adduct ion observed in these reactions and indeed the product ions could also represent a mixture of these isomers. To probe the structure of these ions, the $[M + Li + 48]^+$ and $[M + Na + 48]^+$ reaction products were re-isolated in the ion trap and subjected to structural interrogation by collision (Fig. 3A & B) or ozonolysis (Supplementary material Figure S3). Importantly, these results indicate

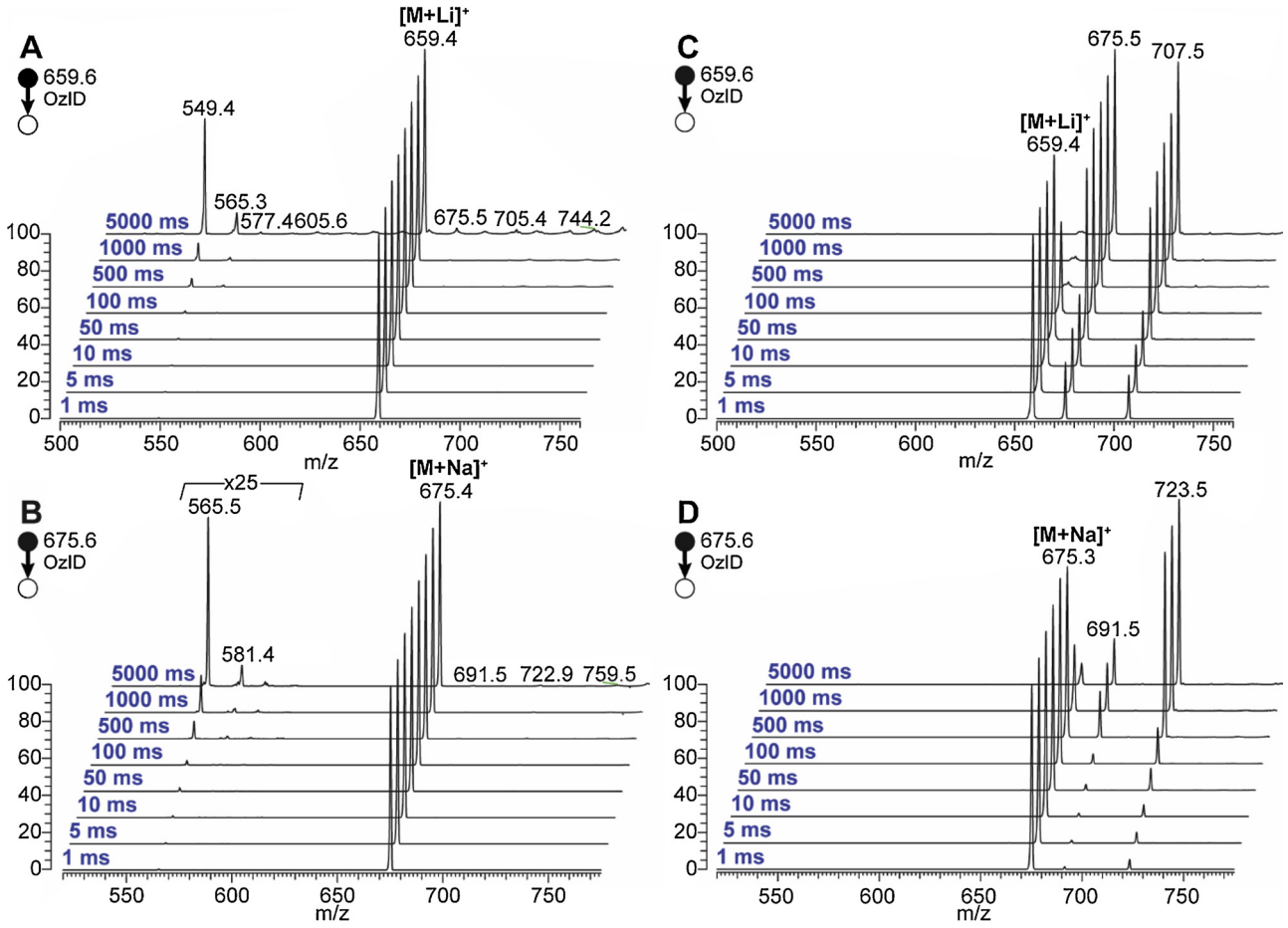

Fig. 2. Mass spectra showing the temporal evolution of product ions from the gas-phase reaction of ozone with cholestanyl oleate as (A) $[M + Li]^+$ or (B) $[M + Na]^+$ and cholesteryl stearate as (C) $[M + Li]^+$ or (D) $[M + Na]^+$. Data are acquired with an ozone concentration of ~4.6×10^{10} molecules cm^{-3} within a linear ion-trap mass spectrometer.

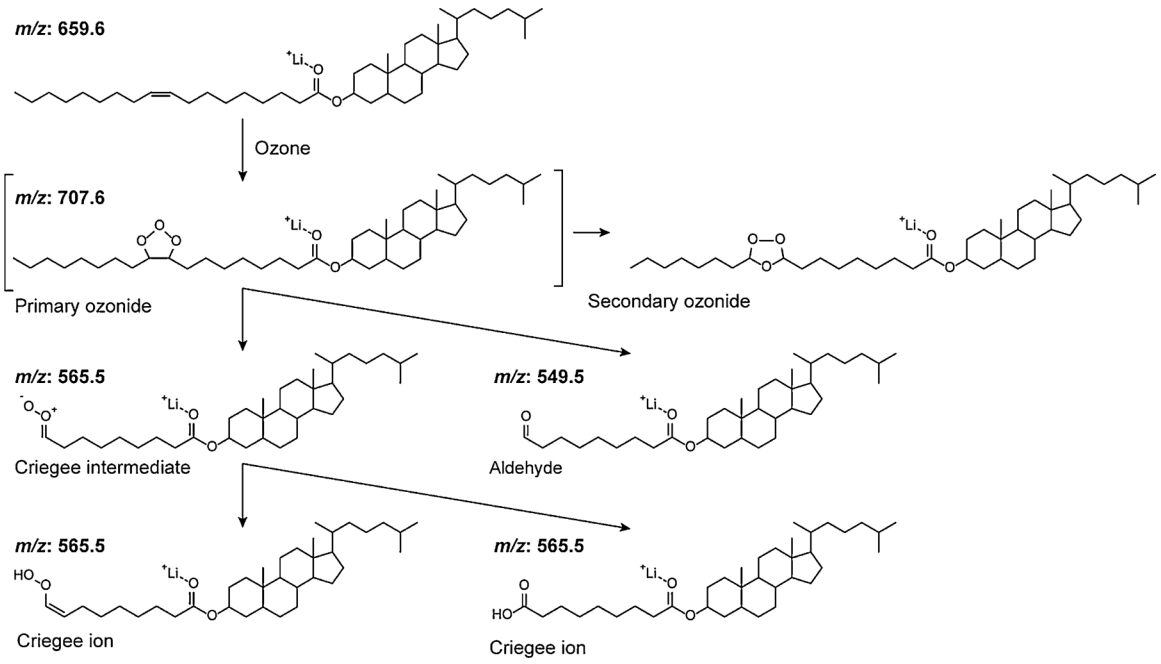

Scheme 1. Proposed reaction scheme for the $[M + Li]^+$ ion of cholestanyl oleate with ozone in the gas phase.

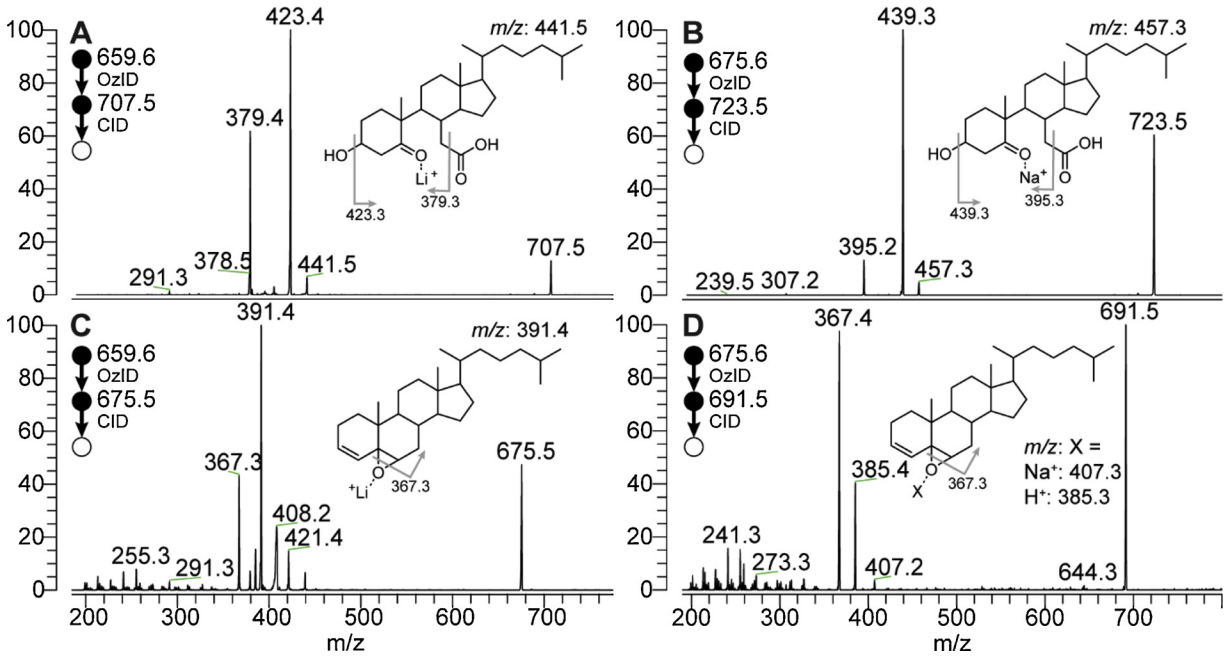

Fig. 3. Sequential OzID/CID of ions generated from the ozonolysis of cholesteryl stearate as either: (A) $[M + Li + 48]^+$, (B) $[M + Na + 48]^+$, (C) $[M + Li + 16]^+$, (D) $[M + Na + 16]^+$. Lithiated cholesteryl stearate OzID/CID spectra were acquired under low ozone conditions (~4.6×10^{10} molecules cm^{-3}), while sodiated OzID/CID spectra were acquired under high ozone conditions (~2.8×10^{11} molecules cm^{-3}).

that the +48 adduct ions are non-reactive towards ozone. This indicates that the vinyl hydroperoxide structures are unlikely as these have previously been shown to undergo facile oxidative cleavage of the carbon-carbon double bond under similar conditions in the gas phase (Vu et al., 2017). At the same time CID of the +48 adduct ions results principly in even-electron product ions, which contrasts with our previous investigations of the unimolecular dissociation of secondary ozonides (Ellis et al., 2017). Rather the spectra in Fig. 3A and B both show abundant product ions resulting from consecutive losses of stearic acid and carbon dioxide (*i.e.*, *m/z* 379 and *m/z* 395, respectively). Loss of carbon dioxide could be rationalised as arising from both the carboxylic acid (**4**) or lactone (**7**) structures indicated in Scheme 2 and makes these the most likely structures to account for the +48 adduct ions observed in the reactions of cholesteryl stearate with ozone.

Prior solution-phase investigations of the reaction of ozone with cholesterol in non-participating solvents (*e.g.*, ethyl acetate) have identified 5,6-epoxides (Gumulka and Smith, 1983) as major reaction products. Similarly, epoxide formation could account for the $[M + Li + 16]^+$ and $[M + Na + 16]^+$ products observed in the gas phase reactions of ionised cholesteryl stearate with ozone (Fig. 2C and D, respectively). Subsequent interrogation of these product ions by CID revealed fragmentation channels consistent with the epoxide structure (Fig. 3C & D), and was comparable to the CID spectrum of an epoxide generated from cholesteryl stearate by solution-phase treatment with *meta*-chloroperbenzoic acid (Supplementary Figure S4). Interestingly, epoxide formation from the ozonolysis of olefins can be accounted for

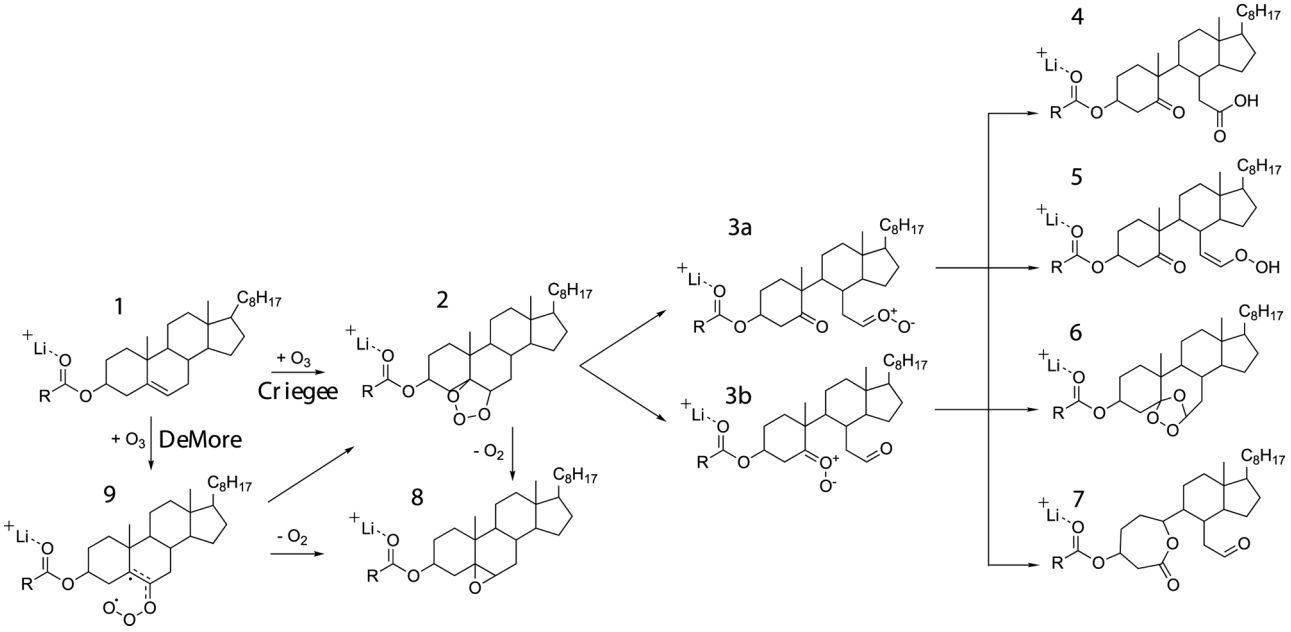

Scheme 2. Proposed reaction manifold for the ozonolysis of endocyclic carbon-carbon double bond in cholesteryl esters **1**.

by two pathways. The first would result from expulsion of dioxygen from the primary ozonide formed by the classical Criegee pathway, while the alternative would invoke an initial diradical intermediate formed as a result of an asymmetric addition of ozone to the alkene (*i.e.*, *via* intermediate **9** in Scheme 2). The latter is sometimes refered to as the DeMore mechanism (Bailey and Lane, 1967; Criegee, 1975; DeMore, 1969). While there is computational evidence that suggests that both mechanisms can compete efficiently in certain unsaturated compounds (Lee and Coote, 2013), unequivocal assignment of the mechanism based on experimental measurements remains a challenge in either the gas or liquid phase. If however, the + 16 Da and + 48 Da reaction products proceed *via* competing mechanisms then one might expect different rates of formation governed by two different transitions states. Careful kinetic analysis of the data presented in Fig. 2 could thus provide important clues as to whether or not all chemistries are governed by a single rate determining step.

3.2. Ozonolysis kinetics of ionised cholestanyl oleate and cholesteryl stearate

The product studies described above suggest that the rate of ozonolysis for a given steryl ester differs between double bonds present in different parts of the molecule. Specifically, the data imply that gas-phase ozonolysis of the endocyclic double bond present within the cholesterol ring system proceeds at a much faster rate than that of the acylic fatty acid alkene. To test this, we performed a series of kinetic experiments (in triplicate) that acquired ozonolysis spectra from cholestanyl oleate or cholesteryl stearate as either $[M + Li]^+$ (Supplementary Material, Figure S5) or $[M + Na]^+$ (Supplementary Material, Figure S6) under low ozone conditions, and derived the pseudo-first order rate constant (k_{1st}) for the reaction of a given steryl ester adduct type with ozone (Table 1). We could then use our empirically derived k_{1st} and the estimated ozone density within the ion trap to calculate the second order rate constant (k_{2nd}) for each reaction.

The kinetic data presented in Table 1 demonstrate that the rate of ozonolysis differs depending on whether the carbon-carbon bond present in the ionised lipid is located within the sterol or fatty acyl chain. For example, reaction of ozone with cholesteryl stearate as an $[M + Li]^+$ ion gave an observed k_{1st} over 30 times higher for that of cholestanyl oleate (Table 1). A similar trend is observed when cholesteryl stearate and cholestanyl oleate are ionised as $[M + Na]^+$. In this instance however, the reaction rate constants between the two isomers differ by only a factor of 6 (Table 1). These results also revealed a significant difference in ozonolysis reaction rate constants for cholesteryl stearate depending on which of the two alkali metal cation adducts was formed. That is, the lithiated cholesteryl stearate has a reaction rate constant 6-times greater than the corresponding sodiated ion. In contrast, the lithiated and sodiated cholestanyl oleate ions gave rise to very similar reaction rate constants within the uncertainty of the measurement. The modulation of ozonolysis rates depending on the cationisation agent has previously been reported for fatty acid methyl esters (FAME). For these much simpler lipids, $[M + Li]^+$ ions underwent gas phase reactions with ozone some 15-times faster than the analogous $[M + Na]^+$ (Pham et al., 2013). This phenomenon could be attributed to greater polarisation of the alkene by lithium compared to sodium cations (Richard Premkumar et al., 2012; Rodgers and Armentrout, 2000) and points to a strong interaction between the charge-carrier and the olefin in the gas phase structure(s) of ionised lipids.

Influence of the metal cation on the carbon-carbon double bond, as described above, could further modulate the ozonolysis product distribution and reaction mechanism. Indeed, the ratio of +16 and + 48 Da product` ions is inverted between the $[M + Li]^+$ and $[M + Na]^+$ cations of the cholesteryl stearate (see Fig. 2). This motivated us to re-analyse the data to determine the product branching ratios for all observed ozonolysis product ions all steryl esters under both alkali metal cation conditions (see Supplementary Material, Table S2). The analysis revealed that, for a given cation, the rate of formation of +16 and + 48 Da product ions was identical; a result consistent with the conclusion that both products are formed through a common transition state (*i.e.*, a single rate determining step). While the product branching ratios do not indicate whether the common transition state is more consistent with a concerted (Criegee, 1975) or step-wise (DeMore, 1969) mechanism, both (1) the importance of the polarisation of the carbon-carbon double bond by the charge-carrier and (2) the abundance of the epoxide product channel suggest that the DeMore mechanism can better account for the experimental observations of ozonolysis of the endocyclic double bond within ionised steryl esters. In an effort to understand the overall efficiency of the gas phase ion-molecule reactions we deployed a widely used point-charge, parameterized trajectory model to estimate collision frequency (Su, 1994). Comparison of the theoretical collision rate with the measured second order rate constant for the lithium adduct ion of cholesteryl stearate gives a reaction efficiency (ϕ) of *ca.* 30%.

Table 1
Rate constants measured on a linear ion-trap mass spectrometer for the gas-phase ozonolysis of cholesteryl esters under low O_3 conditions (~4.6×10^{10} molecules cm^{-3}). Pseudo-first order rates, k_{1st}, were fitted from a minimum of 45 scans for each time point obtained at trapping times ranging.from 0.03 to 5000 ms.

Steryl ester	k_{1st} (s^{-1})	k_{2nd} (cm^3 molec.$^{-1}$ s^{-1}) $\times 10^{-12}$	
$[M + Li]^+$			
Cholestanyl oleate	0.30 (± 0.01)[a]	6.5 (± 0.1)	0.87
Cholesteryl stearate	10.0 (± 0.2)	218 (± 4)	30
Cholesteryl oleate	2.50 (± 0.02)	54.4 (± 0.4)	7.2
$[M + Na]^+$			
Cholestanyl oleate	0.284 (± 0.008)	6.2 (± 0.2)	0.82
Cholesteryl stearate	1.80 (± 0.01)	39 (± 7)	5.2
Cholesteryl oleate	0.720 (± 0.003)	15.66 (± 0.07)	2.1

[a] Errors are 2σ.

3.3. Ozonolysis kinetics and ion-mobility of ionised cholesteryl oleate

To better understand the relationship between carbon-carbon double bond location on the steryl ester and ozonolysis reaction rate, we performed the same series of reactions described above with cholesteryl oleate; a steryl ester that carries double bonds in both positions (Fig. 1C). Mass selection and trapping of cholesteryl oleate as either $[M + Li]^+$ or $[M + Na]^+$ with ozone in a time-dependent manner within the linear ion trap mass spectrometer under low ozone concentration conditions resulted in the mass spectra shown in Fig. 4. These spectra reveal two distinct sets of product ions. The first set of product ions has a *m/z* greater than the precursor ion. They appear +16 and + 48 Da above the precursor and are analogous to products observed from ionised cholesteryl stearate thus indicative of reaction of ozone with the endocyclic double bond present within the cholesteryl ring. The second set of product ions consists of three features below the *m/z* of the precursor ion and are only present at relatively low abundance. The presence of three ions in this mass region contrasts somewhat with the ozonolysis of cholestanyl oleate, during which only a pair of product ions were observed (Fig. 2). The most abundant of these ions was present at 94 Da less than the precursor ion (*m/z* 563 for $[M + Li]^+$ and *m/z* 579 for $[M + Na]^+$), followed by an ion 62 Da less than the precursor ion (*m/z* 595 for $[M + Li]^+$, *m/z* 611 for $[M + Na]^+$; Fig. 4). While the ion 94 Da below the precursor ion can be rationalised by the proposals in Scheme 1, the ion 62 Da lower than the precursor ion does not correspond to any predicted neutral loss for a monounsaturated double bond (see Supplementary material, Table S1). One possible explanation for this feature would be a secondary reaction of the putative endocyclic epoxide at +16. To test this, we re-isolated both the + 16 Da and + 48 Da product ions and subjected them to further ozonolysis

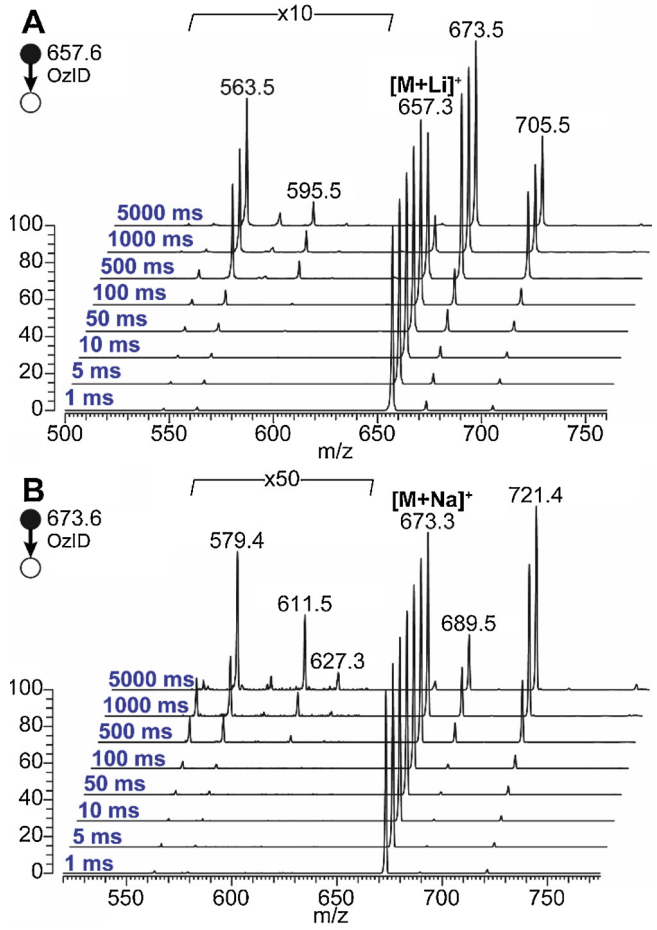

Fig. 4. Time-dependant ozone-induced dissociation (OzID) of cholesteryl oleate as either (A) $[M + Li]^+$ or (B) $[M + Na]^+$ within a modified linear ion trap. Both spectra were acquired under low ozone conditions (~4.6×10^{10} molecules cm^{-3}).

(*i.e.*, OzID/OzID, Fig. 5). For all four conditions (*i.e.* $[M + Li+16]^+$, $[M + Li+48]^+$, $[M + Na+16]^+$ and $[M + Na+48]^+$) a set of two main product ions below the precursor ion mass were produced, each at either 110 Da or 94 Da less than the precursor ion, equating to the predicted aldehyde and Criegee ions arising from the reaction of ozone with the double bond present on oleoyl chain (see Supplementary Material, Table S1). When combined, these aldehyde and Criegee ions produced from OzID/OzID of either the + 16 Da or +48 ion generated from cholesteryl oleate account for all ions observed in the initial OzID mass spectrum (Fig. 4). Additionally, we performed OzID/CID on the ion present at 94 Da less than the precursor ion for both alkali metal cation adducts (Supplementary Figure S8), which produced spectra displaying features of ozonolysis products from both the double bond present in cholesterol (*cf.* Fig. 3) and in fatty acid (*cf.* Supplemental Figures S1 A & S2 A). In summary, all reaction products observed in the gas phase ozonolysis of ionised cholesteryl oleate could be accounted for by Schemes 1 and 2 as either primary or secondary reaction products.

Intriguingly, kinetic analysis of the data in Fig. 4 revealed that the reaction of ozone with ionised cholesteryl oleate was significantly *slower* than that of cholesteryl stearate: 4-times slower for $[M + Li]^+$ and 2.5-times slower for $[M + Na]^+$ (see Table 1). This was entirely unexpected as it might be assumed that the rate of reaction of ozone with cholesteryl oleate could be approximated by the summation of the rates for the analogous cholestanyl oleate and cholesteryl stearate reactions. A possible explanation for this may lie in the site(s) of charge localisation within the steryl ester, with the resulting proximity and availability of the charge activating nearby carbon-carbon double bonds. Given the high oxygen-affinity of alkali metals, the sodium and lithium cations are presumed to be localised to the carbonyl oxygen of the ester that links the fatty acid and sterol. Evidence for this can be seen in the CID mass spectra of lithiated or sodiated sterol esters (Supplemental Figures S1, S2 and S9) that all display prominent product ions corresponding to the cationized fatty acid. If localised on the ester, the alkali metal ions are proximate to the carbon-carbon double bond on the cholesterol moiety of cholesteryl stearate and oleate esters. It follows then that the enhanced rate of ozonolysis in these sterol esters results from the synergistic effects of the intrincisally more reactive endocyclic double bond and polarisation afforded by the nearby charge. However, for ionised cholestanyl and cholesteryl oleate folding of the fatty acyl chain to facilitate through-space charge-olefin interactions should also be considered. Indeed, atomistic modelling of cholesteryl oleate in the liquid phase suggests that a sizeable fraction of structures in the ensemble can be present in a folded state, with the greatest conformational flexibility seen at carbons 3 to 5 on the acyl chain (Heikelä et al., 2006). As a gas phase ion, the folded configuration could bring the *n*-9 double bond nearer to the site of charge localisation on the ester moiety, allowing it to interact with the alkali metal cation. The presence of such compact conformations could establish competitive interactions between the metal ion and the double bonds in the acyl chain and the cholesteryl moiety. This might in turn reduce the inherent

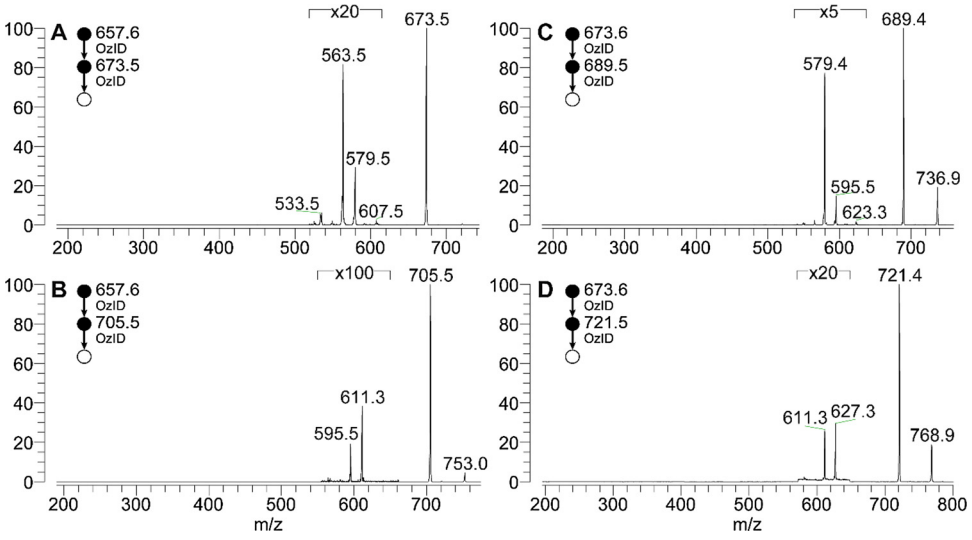

Fig. 5. Sequential OzID/OzID of products arising from the reaction of ozone with the 5,6-double bond present on the cholesterol portion of cholesteryl oleate as either $[M + Li]^+$ (A&B) or $[M + Na]^+$ (C&D). Lithiated OzID/OzID spectra were acquired under low ozone conditions (~4.6×10^{10} molecules cm^{-3}), while sodiated were acquired under high ozone conditions (~2.8×10^{11} molecules cm^{-3}).

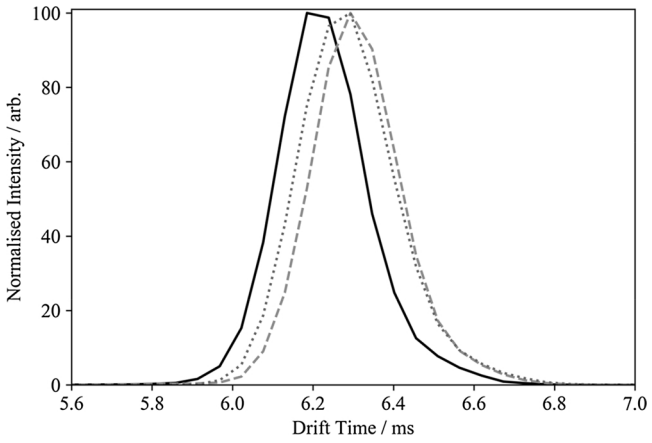

Fig. 6. Arrival time distributions of diagnostic fragment ions (see CID spectra Supplementary Material, Figure S9) from the $[M + Li]^+$ cations of cholestanyl oleate (dotted trace), cholesteryl stearate (dashed trace) and cholesteryl oleate (solid trace) obtained on a travelling wave ion-mobility mass spectrometer. The M + 2 ion of cholesteryl oleate was isolated to mitigate any mass-dependant mobility effects. Collision energy (35 eV) was applied in the transfer region, such that the fragment ions time-align in mobility space with the precursor ions.

reactivity of the cholesterol double bond with ozone and result in the observed attenuation of the ozonolysis rate. Some experimental evidence for this hypothesis can be found in the ion-mobility data present in Fig. 6. Measurements for the $[M + Li]^+$ cations of all three steryl esters (Fig. 1) were undertaken on a travelling wave ion-mobility mass spectrometer. The M + 2 heavy isotope for cholesteryl oleate was mass-selected and used for comparison to the two monounsaturated lipids in order to eliminate any mass-dependent mobility effects. Fig. 6 shows that the arrival time distribution of the isomeric $[M + Li]^+$ cholesteryl stearate and cholestanyl oleate ions are closely aligned (dashed and dotted lines, resepectively). This observation is consistent with these ion ensembles adopting conformations with similar collisional cross sections. In contrast, the $[M + Li]^+$ ion of cholesteryl oleate (solid line) has a significantly shorter arrival time with a distribution centre at 6.2 ms (*cf.* 6.3 ms for the monounsaturated lipid ions). This earlier arrival time distribution is consistent with a compaction of the collisionally averaged geometries of the ion ensemble that could arise from lithium interactions with double bonds present on both the acyl chain and steryl ring.

4. Conclusions

In this study we have used a set of ionised steryl esters with 18-carbon fatty acids to study the gas-phase ozonolysis of acyclic and cyclic carbon-carbon double bonds. Analysis of two structural isomers with the double bond present either in the fatty acyl chain (*i.e.*, cholestanyl oleate) or between carbons 5 and 6 on the B ring of cholesterol (*i.e.*, cholesteryl stearate) revealed disparate reaction products and kinetics. While ozonolysis of ionised cholestanyl oleate was dominated by oxidative cleavage of the fatty acyl moiety, cholesteryl stearate ions were found to undergo addition of one or three oxygens to form putative epoxides and lactones (and/or carboxylic acids), respectively. Interestingly, when compared to previous data, (Barrientos et al., 2017; Ellis et al., 2012; Pham et al., 2013; Poad et al., 2010; Thomas et al., 2008, 2007) there is some evidence that the ratio of $[M + Na + O]^+$ to $[M + Na + O_3]^+$ is higher for endocyclic double bonds than acyclic olefins, suggesting that this ratio could be used analytically as an indicator of unsaturated ring systems. Nevertheless, further investigation is required to characterise this effect as the data presented here indicate that this ratio can also be influenced by other variables including the identity of the cation (*cf.* Fig. 2C and D).

The relative rate of reaction is found to strongly favour the endocyclic double bond with the lithiated cholesteryl stearate having a rate constant measured at more than 30 times faster than the cholestanyl oleate isomer. Surprisingly the reaction of cholesteryl oleate (*i.e.*, a steryl ester with a double bond present in both cholesterol and the fatty acid) with ozone was slower than that of cholesteryl stearate, which we suggest might be due to competition between the cyclic and acyclic carbon-carbon double bonds for an interaction with the site of charge localisation on the steryl ester. Understanding the influence of this competitive interaction and ozonolysis reaction rates may be important from an analytical perspective, particularly since the use of gas-phase ozone for determining double bond position in lipids from biological extracts is becoming increasingly popular (Batarseh et al., 2018; Ellis et al., 2018; Hancock et al., 2018; Poad et al., 2018a, 2018b; Vu et al., 2017).

The reaction of ozone with cholesterol and cholesteryl esters may also be important from a biological perspective, as both lipids are typically present in systems at the air-water interface on external surfaces of the body (*i.e.*, tear film lipid layer, pulmonary surfactant, skin oils, mucous membranes *etc.*).

Acknowledgements

The authors acknowledge support for this research from the Australian Research Council Linkage Project (LP140100711, with industry support from Allergan); Discovery Project (DP150101715) and Future Fellowship schemes (FT110100249, awarded to T.W.M.). S.J.B., and B.L.J.P. acknowledge the support of the Central Analytical Research Facility operated by the Institute for Future Environments (QUT). Cameron Bright (University of Wollongong) is acknowledged for technical assistance. Cholestanyl oleate was donated by Nu-Chek Prep, Inc. (Elysian, MN, USA).

Appendix A. Supplementary data

Supplementary data associated with this article can be found, in the online version, at https://doi.org/10.1016/j.chemphyslip.2018.12.013.

References

Bailey, P.S., Lane, A.G., 1967. Competition between complete and partial cleavage during ozonation of olefins. J. Am. Chem. Soc. 89, 4473–4479. https://doi.org/10.1021/ja00993a040.

Barrientos, R.C., Vu, N., Zhang, Q., 2017. Structural analysis of unsaturated glycosphingolipids using shotgun ozone-induced dissociation mass spectrometry. J. Am. Soc. Mass Spectrom. 28, 2330–2343. https://doi.org/10.1007/s13361-017-1772-2.

Batarseh, A.M., Abbott, S.K., Duchoslav, E., Alqarni, A., Blanksby, S.J., Mitchell, T.W., 2018. Discrimination of isobaric and isomeric lipids in complex mixtures by combining ultra-high pressure liquid chromatography with collision and ozone-induced dissociation. Int. J. Mass Spectrom. 431, 27–36. https://doi.org/10.1016/j.ijms.2018.05.016.

Brown, S.H.J., Mitchell, T.W., Blanksby, S.J., 2011. Analysis of unsaturated lipids by ozone-induced dissociation. Biochim. Biophys. Acta BBA - Mol. Cell Biol. Lipids, Lipidomics Imaging Mass Spectrom. 1811, 807–817. https://doi.org/10.1016/j.bbalip.2011.04.015.

Butovich, I.A., 2013. Tear film lipids. Exp. Eye Res. Tears: A Unique Mucosal Surface Secretion 117, 4–27. https://doi.org/10.1016/j.exer.2013.05.010.

Camera, E., Ludovici, M., Galante, M., Sinagra, J.-L., Picardo, M., 2010. Comprehensive analysis of the major lipid classes in sebum by rapid resolution high-performance liquid chromatography and electrospray mass spectrometry. J. Lipid Res. 51, 3377–3388. https://doi.org/10.1194/jlr.D008391.

Chan, W.T., Hamilton, I.P., 2003. Mechanisms for the ozonolysis of ethene and propene: reliability of quantum chemical predictions. J. Chem. Phys. 118, 1688–1701. https://doi.org/10.1063/1.1531104.

Criegee, R., 1975. Mechanism of ozonolysis. Angew. Chem. Int. Ed. Engl. 14, 745–752. https://doi.org/10.1002/anie.197507451.

Criegee, R., Wenner, G., 1949. Die ozonisierung des 9,10-Oktalins. Justus Liebigs Ann. Chem. 564, 9–15. https://doi.org/10.1002/jlac.19495640103.

DeMore, W.B., 1969. Arrhenius constants for the reactions of ozone with ethylene and acetylene. Int. J. Chem. Kinet. 1, 209–220. https://doi.org/10.1002/kin.550010207.

Dreyfus, M.A., Tolocka, M.P., Dodds, S.M., Dykins, J., Johnston, M.V., 2005. Cholesterol ozonolysis: kinetics, mechanism, and oligomer products. J. Phys. Chem. A 109, 6242–6248. https://doi.org/10.1021/jp050606f.

Ellis, S.R., Hughes, J.R., Mitchell, T.W., Panhuis, Minhet, Blanksby, S.J., 2012. Using ambient ozone for assignment of double bond position in unsaturated lipids. Analyst

137, 1100–1110. https://doi.org/10.1039/C1AN15864C.
Ellis, S.R., Pham, H.T., Panhuis, Minhet, Trevitt, A.J., Mitchell, T.W., Blanksby, S.J., 2017. Radical generation from the gas-phase activation of ionized lipid ozonides. J. Am. Soc. Mass Spectrom. 1–14. https://doi.org/10.1007/s13361-017-1649-4.
Ellis, S.R., Paine, M.R.L., Eijkel, G.B., Pauling, J.K., Husen, P., Jervelund, M.W., Hermansson, M., Ejsing, C.S., Heeren, R.M.A., 2018. Automated, parallel mass spectrometry imaging and structural identification of lipids. Nat. Methods 15, 515–518. https://doi.org/10.1038/s41592-018-0010-6.
Elzhov, T.V., Mullen, K.M., Spiess, A.-N., Bolker, B., 2016. minpack.lm: R Interface to the Levenberg-marquardt Nonlinear Least-squares Algorithm Found in MINPACK, Plus Support for Bounds. R Package Version 1. 2-1. .
Finlayson-Pitts, B., Pitts, J., 2000. Chemistry of the Upper and Lower Atmosphere, 1st edition. Academic Press, San Diego.
Gumulka, J., Smith, L.L., 1983. Ozonization of cholesterol. J. Am. Chem. Soc. 105, 1972–1979. https://doi.org/10.1021/ja00345a052.
Gumulka, J., Pyrek, J.S., Smith, L.L., 1982. Interception of discrete oxygen species in aqueous media by cholesterol: formation of cholesterol epoxides and secosterols. Lipids 17, 197–203. https://doi.org/10.1007/BF02535103.
Hancock, S.E., Ailuri, R., Marshall, D.L., Brown, S.H.J., Saville, J.T., Narreddula, V.R., Boase, N.R., Poad, B.L.J., Trevitt, A.J., Willcox, M.D.P., Kelso, M.J., Mitchell, T.W., Blanksby, S.J., 2018. Mass spectrometry-directed structure elucidation and total synthesis of ultra-long chain (O-acyl)-ω-hydroxy fatty acids. J. Lipid Res. 59, 1510–1518. https://doi.org/10.1194/jlr.M086702. jlr.M086702.
Heikelä, M., Vattulainen, I., Hyvönen, M.T., 2006. Atomistic simulation studies of cholesteryl oleates: model for the core of lipoprotein particles. Biophys. J. 90, 2247–2257. https://doi.org/10.1529/biophysj.105.069849.
Hirabayashi, T., Anjo, T., Kaneko, A., Senoo, Y., Shibata, A., Takama, H., Yokoyama, K., Nishito, Y., Ono, T., Taya, C., Muramatsu, K., Fukami, K., Muñoz-Garcia, A., Brash, A.R., Ikeda, K., Arita, M., Akiyama, M., Murakami, M., 2017. PNPLA1 has a crucial role in skin barrier function by directing acylceramide biosynthesis. Nat. Commun. 8, 14609. https://doi.org/10.1038/ncomms14609.
Hutchins, P.M., Moore, E.E., Murphy, R.C., 2011. Electrospray MS/MS reveals extensive and nonspecific oxidation of cholesterol esters in human peripheral vascular lesions. J. Lipid Res. 52, 2070–2083. https://doi.org/10.1194/jlr.M019174.
Jaworski, K., Smith, L.L., 1988. Ozonization of cholesterol in nonparticipating solvents. J. Org. Chem. 53, 545–554. https://doi.org/10.1021/jo00238a014.
Khairallah, G.N., Maccarone, A.T., Pham, H.T., Benton, T.M., Ly, T., da Silva, G., Blanksby, S.J., O'Hair, R.A.J., 2015. Radical formation in the gas-phase ozonolysis of deprotonated cysteine. Angew. Chem. Int. Ed. 54, 12947–12951. https://doi.org/10.1002/anie.201506019.
Krisyuk, B.E., Maiorov, A.V., Mamin, E.A., Popov, A.A., 2013. Calculation of the effect of double bond strain in 1-chloroethylene and 1,1-dichloroethylene on the rate and mechanism of their reactions with ozone. React. Kinet. Catal. Lett. 54, 149–156. https://doi.org/10.1134/S0023158413020092.
Krisyuk, B.E., Maiorov, A.V., Popov, A.A., 2016. Kinetics and mechanism of ozone addition to olefins and dienes. React. Kinet. Catal. Lett. 57, 326–332. https://doi.org/10.1134/S0023158416030083.
Lee, R., Coote, M.L., 2013. New insights into 1,2,4-trioxolane stability and the crucial role of ozone in promoting polymer degradation. Phys. Chem. Chem. Phys. 15, 16428–16431. https://doi.org/10.1039/C3CP52863D.
Lide, D.R., 2005. Dipole moments. CRC Handbook of Chemistry and Physics, Internet Version. CRC Press, Boca Raton, FL.
Maiorov, A.V., Krisyuk, B.E., Popov, A.A., 2008. The reaction of ozone with hexafluoropropylene: competition of concerted and nonconcerted addition. Russ. J. Phys. Chem. B 2, 707–710. https://doi.org/10.1134/S1990793108050084.
Marshall, D.L., Saville, J.T., Maccarone, A.T., Ailuri, R., Kelso, M.J., Mitchell, T.W., Blanksby, S.J., 2016. Determination of ester position in isomeric (O-acyl)-hydroxy fatty acids by ion trap mass spectrometry. Rapid Commun. Mass Spectrom. 30, 2351–2359. https://doi.org/10.1002/rcm.7715.
Miller, T.M., 2005. Atomic and molecular polarizabilities. CRC Handbook of Chemistry and Physics, Internet Version. CRC Press, Boca Raton, FL.
Monks, P.S., Archibald, A.T., Colette, A., Cooper, O., Coyle, M., Derwent, R., Fowler, D., Granier, C., Law, K.S., Mills, G.E., Stevenson, D.S., Tarasova, O., Thouret, V., von Schneidemesser, E., Sommariva, R., Wild, O., Williams, M.L., 2015. Tropospheric ozone and its precursors from the urban to the global scale from air quality to short-lived climate forcer. Atmos. Chem. Phys. 15, 8889–8973. https://doi.org/10.5194/acp-15-8889-2015.
Nelson, D.L., Cox, M.M., 2008. Lehninger Principles of Biochemistry, 5th ed. W. H. Freeman and Company, New York, NY, USA.
Paryzek, Z., Martynow, J., Swoboda, W., 1990. Reaction of ozone with steroidal allylic alcohols: evidence for intramolecular interception of the 'Criegee carbonyl/carbonyl oxide intermediate. J. Chem. Soc. Perkin Trans. I 1, 1220–1221. https://doi.org/10.1039/P19900001220.
Pham, H.T., Maccarone, A.T., Campbell, J.L., Mitchell, T.W., Blanksby, S.J., 2013. Ozone-induced dissociation of conjugated lipids reveals significant reaction rate enhancements and characteristic odd-electron product ions. J. Am. Soc. Mass Spectrom. 24, 286–296. https://doi.org/10.1007/s13361-012-0521-9.
Poad, B.L.J., Pham, H.T., Thomas, M.C., Nealon, J.R., Campbell, J.L., Mitchell, T.W., Blanksby, S.J., 2010. Ozone-induced dissociation on a modified tandem linear ion-trap: observations of different reactivity for isomeric lipids. J. Am. Soc. Mass Spectrom. 21, 1989–1999. https://doi.org/10.1016/j.jasms.2010.08.011.
Poad, B.L.J., Maccarone, A.T., Yu, H., Mitchell, T.W., Saied, E.M., Arenz, C., Hornemann, T., Bull, J.N., Bieske, E.J., Blanksby, S.J., 2018a. Differential-mobility spectrometry of 1-Deoxysphingosine isomers: new insights into the gas phase structures of ionized lipids. Anal. Chem. 90, 5343–5351. https://doi.org/10.1021/acs.analchem.8b00469.
Poad, B.L.J., Zheng, X., Mitchell, T.W., Smith, R.D., Baker, E.S., Blanksby, S.J., 2018b. Online ozonolysis combined with ion mobility-mass spectrometry provides a new platform for lipid isomer analyses. Anal. Chem. 90, 1292–1300. https://doi.org/10.1021/acs.analchem.7b04091.
Prendergast, M.B., Kirk, B.B., Savee, J.D., Osborn, D.L., Taatjes, C.A., Masters, K.-S., Blanksby, S.J., da Silva, G., Trevitt, A.J., 2016. Formation and stability of gas-phase o-benzoquinone from oxidation of ortho-hydroxyphenyl: a combined neutral and distonic radical study. Phys. Chem. Chem. Phys. 18, 4320–4332. https://doi.org/10.1039/C5CP02953H.
Pryor, W.A., Houk, K.N., Foote, C.S., Fukuto, J.M., Ignarro, L.J., Squadrito, G.L., Davies, K.J.A., 2006. Free radical biology and medicine: it's a gas, man! Am. J. Physiol. Regul. Integr. Comp. Physiol. 291, R491–511. https://doi.org/10.1152/ajpregu.00614.2005.
Pulfer, M.K., Murphy, R.C., 2004. Formation of biologically active oxysterols during ozonolysis of cholesterol present in lung surfactant. J. Biol. Chem. 279, 26331–26338. https://doi.org/10.1074/jbc.M403581200.
Pulfer, M.K., Harrison, K., Murphy, R.C., 2004. Direct electrospray tandem mass spectrometry of the unstable hydroperoxy bishemiacetal product derived from cholesterol ozonolysis. J. Am. Soc. Mass Spectrom. 15, 194–202. https://doi.org/10.1016/j.jasms.2003.10.011.
Pulfer, M.K., Taube, C., Gelfand, E., Murphy, R.C., 2005. Ozone exposure in vivo and formation of biologically active oxysterols in the lung. J. Pharmacol. Exp. Ther. 312, 256–264. https://doi.org/10.1124/jpet.104.073437.
Richard Premkumar, J., Vijay, D., Narahari Sastry, G., 2012. The significance of the alkene size and the nature of the metal ion in metal–alkene complexes: a theoretical study. Dalton Trans. 41, 4965–4975. https://doi.org/10.1039/C2DT30119A.
Rodgers, M.T., Armentrout, P.B., 2000. Noncovalent metal–ligand bond energies as studied by threshold collision-induced dissociation. Mass Spectrom. Rev. 19, 215–247. https://doi.org/10.1002/1098-2787(200007)19:4<215::AID-MAS2>3.0.CO;2-X.
Ronsein, G.E., Prado, F.M., Mansano, F.V., Oliveira, M.C.B., Medeiros, M.H.G., Miyamoto, S., Di Mascio, P., 2010. Detection and characterization of cholesterol-oxidized products using HPLC coupled to dopant assisted atmospheric pressure photoionization tandem mass spectrometry. Anal. Chem. 82, 7293–7301. https://doi.org/10.1021/ac1011987.
Spiess, A.-N., 2016. Propagate: Propagation of Uncertainty. R Package Version 1. pp. 0–6.
Su, T., 1994. Parametrization of kinetic energy dependences of ion–polar molecule collision rate constants by trajectory calculations. J. Chem. Phys. 100https://doi.org/10.1063/1.466255. 4703–4703.
Teiwes, R., Elm, J., Handrup, K., Jensen, E.P., Bilde, M., Pedersen, H.B., 2018. Atmospheric chemistry of iodine anions: elementary reactions of I−, IO−, and IO2− with ozone studied in the gas-phase at 300 K using an ion trap. Phys. Chem. Chem. Phys. 20, 28606–28615. https://doi.org/10.1039/C8CP05721D.
Thomas, M.C., Mitchell, T.W., Harman, D.G., Deeley, J.M., Murphy, R.C., Blanksby, S.J., 2007. Elucidation of double bond position in unsaturated lipids by ozone electrospray ionization mass spectrometry. Anal. Chem. 79, 5013–5022. https://doi.org/10.1021/ac0702185.
Thomas, M.C., Mitchell, T.W., Harman, D.G., Deeley, J.M., Nealon, J.R., Blanksby, S.J., 2008. Ozone-induced dissociation: elucidation of double bond position within mass-selected lipid ions. Anal. Chem. 80, 303–311. https://doi.org/10.1021/ac7017684.
Vu, N., Brown, J., Giles, K., Zhang, Q., 2017. Ozone-induced dissociation on a traveling wave high-resolution mass spectrometer for determination of double-bond position in lipids. Rapid Commun. Mass Spectrom. 31, 1415–1423. https://doi.org/10.1002/rcm.7920.
Wentworth, P., Nieva, J., Takeuchi, C., Galve, R., Wentworth, A.D., Dilley, R.B., DeLaria, G.A., Saven, A., Babior, B.M., Janda, K.D., Eschenmoser, A., Lerner, R.A., 2003. Evidence for ozone formation in human atherosclerotic arteries. Science 302, 1053–1056. https://doi.org/10.1126/science.1089525.
Zhou, S., Forbes, M.W., Katrib, Y., Abbatt, J.P.D., 2016. Rapid oxidation of skin oil by ozone. Environ. Sci. Technol. Lett. 3, 170–174. https://doi.org/10.1021/acs.estlett.6b00086.